The Downtown Review

Volume 1 | Issue 1 Article 6

2015

On the Detection of Exoplanets via Radial Velocity Doppler Spectroscopy

Joseph P. Glaser
Cleveland State University

1 Introduction to Exoplanets

For centuries, some of humanity's greatest minds have pondered over the possibility of other worlds orbiting the uncountable number of stars that exist in the visible universe. The seeds for eventual scientific speculation on the possibility of these "exoplanets" began with the works of a 16$^{\text{th}}$ century philosopher, Giordano Bruno. In his modernly celebrated work, *On the Infinite Universe & Worlds*, Bruno states: "This space we declare to be infinite (...) In it are an infinity of worlds of the same kind as our own." By the time of the European Scientific Revolution, Isaac Newton grew fond of the idea and wrote in his *Principia*: "If the fixed stars are the centers of similar systems [when compared to the solar system], they will all be constructed according to a similar design and subject to the dominion of One." Due to limitations on observational equipment, the field of exoplanetary systems existed primarily in theory until the late 1980s.

The latter half of the 20$^{\text{th}}$ century brought forward a number of technological innovations in astronomy. These improvements on ground-based observational equipment allowed astrophysicists the ability to revisit the possibility of exoplanets. In 1988, a team of researchers at the University of Victoria and the University of British Colombia discovered the first exoplanet, Gamma Cephei Ab, through the use of astrometry and radial velocity techniques similar to that used today. However, the planet's existence could not be accurately confirmed until 2002, leading to the claim of the first confirmed discovery to be shifted to the discoverers of PSR B1257+12 B & C in 1992. In the decades since, astrophysicists and astronomers across the globe have developed an array of methodologies to discover many more of these extrasolar worlds. As these discoveries continue to dot the scientific headlines and push the limits of observational astronomy, it is important for the non-astrocentric fields of physics to understand the scientific backbone supporting these discoveries. It is the hope of the author that the contents of this article will aid in demystifying this new frontier and encourage others to join the hunt.

2 Overview of Terminology

To begin, we will define exactly what it means for a stellar companion to be considered an *exoplanet*. In 2003, the Working Group on Extrasolar Planets (WGESP) of the International Astronomical Union (IAU) modified its definition of sub-stellar companions to be defined as:

> Objects with true masses below the limiting mass for thermonuclear fusion of deuterium (currently calculated to be 13 Jupiter masses for objects of solar metallicity) that orbit stars or stellar remnants are "planets" (no matter how they formed). The minimum mass/size required for an extrasolar object to be considered a planet should be the same as that used in our Solar System.

Thus, when we discuss these discoveries it is important to keep in mind the maximum size of the sub-stellar companions we consider to be exoplanets. Other objects commonly discussed by researchers in the field are defined as:

> Substellar objects with true masses above the limiting mass for thermonuclear fusion of deuterium are "brown dwarfs", no matter how they formed nor where they are located.
>
> Free-floating objects in young star clusters with masses below the limiting mass for thermonuclear fusion of deuterium are not "planets", but are "sub-brown dwarfs" (or whatever name is most appropriate).

Once discovered and classified into one of the three above categories, the exoplanets must be named. Before confirmation by other research teams, exoplanets retain the name designated by the nomenclature of the experiment (e.g. Keppler-19c). After confirmation, the creation of a naming standard is the subject of current debate within the IAU. For simplicity's sake, the reader should recognize the following naming guidelines presented by Hessman *et al.* (2010) as an acceptable standard:

1. The formal name of an exoplanet is obtained by appending the appropriate suffixes to the formal name of the host star or stellar system. The upper hierarchy is defined by upper-case letters, followed by lower-case letters, followed by numbers, etc. The naming order within a hierarchical level is for the order of discovery only.

2. Whenever the leading capital letter designation is missing, this is interpreted as being an informal form with an implicit unless otherwise explicitly stated.

3. As an alternative to the nomenclature standard in #1, a hierarchical relationship can be expressed by concatenating the names of the higher order system and placing them in parentheses, after which the suffix for a lower order system is added.

4. When in doubt (i.e. if a different name has not been clearly set in the literature), the hierarchy expressed by the nomenclature should correspond to dynamically distinct (sub-)systems in order of their dynamical relevance. The choice of hierarchical levels should be made to emphasize dynamical relationships, if known.

For more information regarding core-terminology or conventions central to astronomy, it is suggested for the reader to review astronomical introductory texts, such as Frank Shu's *The Physical Universe: An Introduction to Astronomy* or Robert Baker's *Astronomy*. For an informative read on detection methods and their own terminology other than the Iodine Cell technique described later in this article, the author suggests the review Sara Seager's *Exoplanets* and related texts by the University of Arizona Press.

3 The Two Body Problem

A fundamental part of constructing our detection method is ability to translate the "wobble" of a star into the orbital information of its sub-stellar companion(s). For simplicity's sake, we will only consider the case of a singular companion for the entirety of this paper. For a more detailed description of multi-planet systems, the author suggests the review of the numerical methodology employed by Beaugé *et al.* (2012).

Consider a star, M_s, with a planet, M_p, in orbit around it. It is well known to any undergraduate in physics that by converting coordinate systems to that of the reference frame of the stationary center of mass, the two-body problem reduces to that of a single body moving within a potential well. We do this by stating:

$$\vec{r}_{cm} = \frac{M_p\vec{r}_p + M_s\vec{r}_s}{M_s + M_p} \tag{1}$$

$$\vec{r} = \vec{r}_s - \vec{r}_p \tag{2}$$

with $\vec{r}_s$ being the position vector of star from the origin, $\vec{r}_p$ being the position vector of the planet, $\vec{r}$ being the difference in position vectors, and $\vec{r}_{cm}$ being the vector pointing to the center of mass from the origin. Without loss of generality, we may set $\vec{r}_{cm} = 0$. Combining this fact with Eq. 1 & Eq. 2 yields the following relationships:

$$\vec{r}_s = \frac{M_p}{M_s + M_p}\vec{r} \tag{3}$$

$$\vec{r}_p = -\frac{M_s}{M_s + M_p}\vec{r} \tag{4}$$

Thus, if we know $\vec{r}$, which is the solution to the equivalent Lagrange one-body problem, we can solve for the individual motions of the star and the planet.

When considering a planet orbiting in a plane parallel to the XY-plane, we express $\vec{r}$ in the following manner:

$$\vec{r} = \frac{a(1-e^2)}{1+e\cos f}\begin{pmatrix}\cos f\\ \sin f\\ 0\end{pmatrix} \tag{5}$$

where a is the semi-major axis, e is the eccentricity, and $f = \theta - \varpi$ is the true anomaly[1]. However, this implies that the observation axis is that of the orbital plane's Z-axis. In most cases, the plane of the orbit has been rotated about each of the observation axes individually. We can represent this coordinate transformation under rotations about an axis by the following linear transforms:

$$\boldsymbol{P}_x(\phi) = \begin{bmatrix}1 & 0 & 0\\ 0 & \cos\phi & -\sin\phi\\ 0 & \sin\phi & \cos\phi\end{bmatrix} \tag{6}$$

$$\boldsymbol{P}_z(\phi) = \begin{bmatrix}\cos\phi & -\sin\phi & 0\\ \sin\phi & \cos\phi & 0\\ 0 & 0 & 1\end{bmatrix} \tag{7}$$

Allowing our orientation angles to be i, Ω, & ω, we can summarize the coordinate transformation from the orbital plane (x, y, z) to the observer's plane (x_{ob}, y_{ob}, z_{ob}) as the product of three rotations:

1. The rotation about the z-axis through the angle ω to align the periapse with the ascending node.
2. The rotation about the x'-axis through the angle i to allow the orbital plane and the observer's plane to be parallel.
3. The rotation about the z''-axis through the angle Ω to align the periapse with the x_{ob}-axis.

Thus, our transform is of the form:

$$\vec{r}_{ob} = \boldsymbol{P}_z(\Omega)\boldsymbol{P}_x(i)\boldsymbol{P}_z(\omega)\vec{r} \tag{8}$$

And we arrive with:

$$\vec{r}_{ob} = \frac{a(1-e^2)}{1+e\cos f}\begin{pmatrix}\cos\Omega\cos\psi - \sin\Omega\sin\psi\cos i\\ \sin\Omega\cos\psi + \cos\Omega\sin\psi\cos i\\ \sin\psi\sin i\end{pmatrix} \tag{9}$$

with $\psi = \omega + f$. This is useful because we can now accurately describe any planetary system's orientation towards our line of sight and the sky's reference frame.

With the ability to describe an orbit about the center of mass of either body, we can now continue towards deriving the radial velocity equation. This will allow us to relate our observations to the parameters of the sub-stellar companion's orbit. The radial velocity of the star can be expressed as:

$$v_r = \dot{\vec{r}}_s \cdot \hat{z}_{ob} = V_{cm,z} + \frac{M_p}{M_s + M_p}\dot{r}_{ob,z} \tag{10}$$

where $V_{cm,z}$ is the magnitude of the velocity vector of the barycenter relative to the observer and $\dot{r}_{ob,z} = \dot{\vec{r}}_{ob} \cdot \hat{z}_{ob}$ is the velocity of $\vec{r}_{ob}$ projected onto the z_{ob}-axis. We now obtain that:

$$\dot{r}_{ob,z} = \dot{r}\sin\psi\sin i + r\dot{f}\cos\psi\sin i \tag{11}$$

[1]It should be noted that the true anomaly being expressed here is a function of the current angular position, θ, and the longitude of periapse, ϖ. There are other methods of expression, but this is the most common, regardless of its difficulty of measurement.

Next, we obtain $\dot{r}$ by taking the derivative with respect to time:

$$\dot{r} = \frac{a(1-e^2)}{1+e\cos f} \cdot \frac{\dot{f}e\sin f}{1+e\cos f} = \frac{r\dot{f}e\sin f}{1+e\cos f} \tag{12}$$

Noting Kepler's Second and Third Laws, we know that:

$$L = \frac{2\pi}{T}a^2\sqrt{1-e^2} = r^2\dot{f} \tag{13}$$

After some algebra is done, we obtain:

$$r\dot{f} = \frac{2\pi}{T}\frac{a}{\sqrt{1-e^2}}(1+e\cos f) \tag{14}$$

Making use of Eq. 12 & 14, we are left with:

$$\dot{r}_{ob,z} = \frac{2\pi}{T}\frac{a\sin i}{\sqrt{1-e^2}}(\cos\psi + e\cos\omega) \tag{15}$$

We can now finally write our final form of the radial velocity equation as:

$$v_r = V_{cm,z} + K(\cos\psi + e\cos\omega) \tag{16}$$

where:

$$K = \frac{2\pi}{T}\frac{M_p\sin i}{M_s+M_p}\frac{a}{\sqrt{1-e^2}} \tag{17}$$

Thus, we now have a model which relates the measurable radial velocity and mass of the star to the parameters of its sub-stellar companion's orbit: the period T; the minimum mass $M_p\sin i$; the semi-major axis a; and the eccentricity e.

4 The Relativistic Doppler Shift

It is a great triumph of physics to be able to utilize the radial velocity of a star to detect the presence of sub-stellar companions. However, to have the precision needed to measure the effects on the parent star, we need a technique stronger than that of astrometry[2]. In order to retrieve this information, we utilize the relativistic Doppler effect.

We know that the general Lorentz transforms for a frame S' moving at a velocity $\vec{V}$ with respect to the frame S is given by:

$$\vec{R}' = \vec{R} + (\gamma-1)\frac{(\vec{R}\cdot\vec{\beta})\vec{\beta}}{||\beta||^2} - \gamma\vec{\beta}ct \tag{18}$$

$$ct' = \gamma(ct - \vec{\beta}\cdot\vec{R}) \tag{19}$$

with $\vec{\beta} = \vec{V}c^{-1}$ and $\gamma = \sqrt{1-||\vec{\beta}||^2}^{-1}$, as per the usual convention.

Let us now imagine a plane wave of light is emitted in the S rest frame, denoted as $e^{i(\vec{k}\cdot\vec{R}-2\pi\nu t)}$, at the position $\vec{R}$. Now, allow an observer in the moving S' frame to be looking at the light along the $\hat{k}'$ direction

[2]Astrometry is a statistical branch of astronomy which focuses on optically measuring and recording the movements of celestial bodies in the night sky to high precision.

in his rest frame. The observer would measure the emitted wave as having the form $e^{i(\vec{k}'\cdot\vec{R}'-2\pi\nu' t)}$. Thus, we can substitute the Lorentz transforms into the phase equation of the light and retrieve:

$$\vec{k}'\cdot\left[\vec{R}+(\gamma-1)\frac{(\vec{R}\cdot\vec{\beta})\vec{\beta}}{||\vec{\beta}||^2}-\gamma\vec{\beta}ct\right]-\frac{2\pi\nu'}{c}\left[\gamma(ct-\vec{\beta}\cdot\vec{R})\right] \tag{20}$$

Note that when the plane wave is viewed in the source's S frame, it has the form $e^{i(\vec{k}\cdot\vec{R}-2\pi\nu t)}$. Thus, we can separate the spacial and temporal parts of the equation to find:

$$\vec{R}\cdot\underbrace{\left[\vec{k}'+\gamma(\vec{k}'\cdot\vec{\beta})\frac{\vec{\beta}}{||\vec{\beta}||^2}+\gamma||\vec{k}'||\vec{\beta}\right]}_{\vec{k}} \tag{21}$$

for the spacial part and:

$$-t\underbrace{[2\pi\nu'\gamma((\hat{k}'\cdot\vec{\beta})+1)]}_{2\pi\nu} \tag{22}$$

for the temporal part. Therefore, an observer in the S' frame, which sees the light source in the S frame moving at a relative velocity of $\vec{V}$, will measure the Doppler shift to be:

$$\frac{\nu}{\nu'}=\frac{\lambda'}{\lambda}=\gamma(1+\hat{k}'\cdot\vec{\beta}) \tag{23}$$

For the case related to exoplanets, we have the ability to approximate $\hat{k}'\cdot\vec{\beta}$ as equal to v_r. This is because if the distance to the source's barycenter is on the order of light years and the orbit's semi-major axis is on the order of AU, then $\vec{k}'_{z'} >> \vec{k}'_{x'}, \vec{k}'_{y'}$ and thus $\hat{k}' \approx \hat{z}_{ob}$. In addition, if one is interested in low-amplitude variations in v_r of more than 0.1 m s^{-1}, the relativistic term can be dropped. This allows us to neglect the need to measure the transverse velocity of the star, which would require direct observation methods. Thus, we find that the radial velocity of a star is related to the Doppler shift of its received spectrum by:

$$v_r = c\frac{\lambda'-\lambda}{\lambda} = c(z-1) \tag{24}$$

where $z=\frac{\lambda'}{\lambda}$ is the Doppler parameter.

5 Instrumentation

Depending on the precision needed to break the noise threshold in the radial velocity measurements, the design of instrumentation is key to detecting less-massive exoplanets. To give the reader an understanding of the precision needed to discover exoplanets, consider the following:

> For an observer on Earth to detect an exoplanet with the mass and orbit of Jupiter around a sun-like star, they would need to resolve a radial velocity semi-amplitude of $K = 12.7$ m s^{-1}. For a Neptunian planet orbiting at $a = 0.1$ AU, one would need to resolve $K = 4.8$ m s^{-1}. Finally, to detect an exact duplicate of Earth around another sun-like star, the observer would need to resolve $K = 0.09$ m s^{-1}.

In order to achieve a precision of just 3 m s^{-1}, a measurement of wavelength shifts on the order of femtometers is required. Measurements at that scale must be done through the use of multiple intense spectral lines with

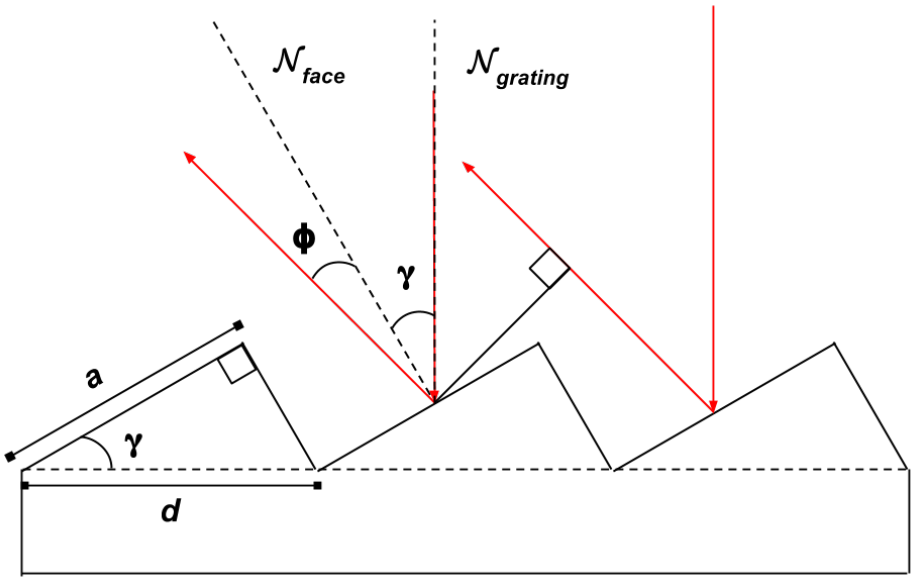

Figure 1: The diagram for an echelle grating of blaze angle γ and face-length d. The normals of the face and grating surfaces are shown along with sample light rays.

low amounts of line broadening. Since most stars are comprised of many elements at high temperatures and pressures, significant broadening and mixing of the spectrum occurs. To combat this, a method proposed by Butler *et al.* (1996) allows for the observed star-light to pass through an iodine cell before entering the optics of the telescope. By doing so, the stellar spectrum is multiplied by the intense spectrum of iodine, allowing for fine Doppler shifts in the peak wavelengths to be measured. It is important that the line broadening of the iodine spectrum be kept at a minimum, which is successfully achieved by constructing a cell similar to that described by Marcy & Butler (1992).

In addition, the method requires high resolution spectrometers ($R \geq 50,000$) that also allow for high intensity efficiency and coverage over a large spectral range. This requirement has lead to the wide use of echelle spectrometers in experiments requiring high velocity precision. The detailed description of this is detailed in the following subsection.

With regards to ground-based telescope observations, such as those done during the Lick Iodine Planet Search, other considerations much be taken into consideration to lower the noise threshold of the observed stellar spectrum. The effects of a change in air temperature of 0.1^{o}K is sufficient to introduce an error of 1 m s^{-1} into the experiment (Lovis *et al.* 2010). Telescope optics must be chosen in such a way as to reduce thermal expansion variations during exposures. The CCD array being used to record the out-put of the spectrometer must also maintain thermal stability as well as pixel-pixel uniformity. Ultimately, these and other errors alter the point-spread function (PSF) of the instrument during an exposure, which can lead to disastrous effects during analysis.

5.1 The Echelle Grating

The center piece of the echelle spectrometer is the echelle grating: a type of blazed reflection grating. A diagram of this type of grating can be found in Figure 1. Since knowing the point-spread function (PSF) of the instrumentation will become vital to precisely measuring the Doppler parameter, it is worth deriving

the contribution of the echelle grating itself. Not only will this showcase why the grating is used in the spectrograph, but also allow us to understand exactly how it works.

Let us imagine shining monochromatic light, emanating from a point-source, at the echelle grating. The length of the grating faces will be d and the blaze angle will be γ. Allow the light rays to hit the grating at the center of each face and at the angle $\theta_i \approx \gamma$. Then the problem of finding the intensity pattern of the reflected light (in this case, the PSF) breaks down into two parts: the interference of the light waves and the diffraction of the light waves around the blazed edges of the grating faces.

First, we shall attack the interference problem. For an echelle grating, the derivation is that of an n-slit transmission grating of "slit width" of d. The total electric field at a screen in the far field is:

$$E = E_0 \sum_{j=1}^{N} e^{i(2j\alpha_I)} = E_0 \frac{\sin(N\alpha_I)}{\sin \alpha_I} \tag{25}$$

where $\alpha_I = \frac{\pi}{\lambda} d(\sin\theta_i + \sin\theta_o)$ is the phase difference due to different path lengths. Thus, the normalized intensity due to interference is:

$$I_I(\lambda, \theta_o) = \frac{\sin^2[\frac{\pi}{\lambda} L(\sin\theta_i + \sin\theta_o)]}{\sin^2[\frac{\pi}{\lambda} d(\sin\theta_i + \sin\theta_o)]} \tag{26}$$

Now we will tackle the problem of diffraction of the light rays around the blazed edges of the grating. As before we will only be allowing the angle $\theta_i \approx \gamma$. Given this condition, the electric field at a screen in the far field is:

$$E_B = E_0 \frac{\sin \alpha_B}{\alpha_B} \tag{27}$$

where $\alpha_B = \frac{\pi}{\lambda}(d\cos\gamma)(\sin\theta_i' + \sin\theta_o')$ is the phase difference, $\theta_i' = \theta_i - \gamma$ and $\theta_o' = \theta_o - \gamma$. Therefore, the normalized intensity due to diffraction is:

$$I_B(\lambda, \theta_o) = \frac{\sin^2[\frac{\pi}{\lambda}(d\cos\gamma)(\sin\theta_i' + \sin\theta_o')]}{[\frac{\pi}{\lambda}(d\cos\gamma)(\sin\theta_i' + \sin\theta_o')]^2} \tag{28}$$

Equation 28 is referred to as the "blaze function" in most literature and allows for the central maximum to be shifted to a higher order based on the blaze angle, γ.

We now combine the two products through an algebra trick involving the diffraction grating equation. The goal is to find a relationship $\frac{d}{\lambda}$ in the interference case and substitute it into α_B to find the total intensity. We do this by:

$$\begin{aligned} n\lambda &= d(\sin\theta_i + \sin\theta_o) \\ &= d(\sin(\theta_i' + \gamma) + \sin(\theta_o' + \gamma)) \\ &= d(2\sin\gamma\cos\theta_i') \quad \text{when } \theta_i' = -\theta_o' \end{aligned}$$

$$\frac{d}{\lambda} = \frac{n}{2\sin\gamma\cos\theta_i'} \tag{29}$$

Substituting Equation 29 into our relationship for α_B, we arrive at final form for the PSF due to an echelle grating:

$$I(n, \theta_o') = \mathrm{sinc}^2\left[\frac{n\pi(\sin\theta_i' + \sin\theta_o')}{2\tan\gamma\cos\theta_o'}\right] \tag{30}$$

This final form allows us to see the echelle grating's primary purpose. For each wavelength, the grating shifts the central maximum out from the first order and into to another higher order. The order to which it then resides is dependent on the physical characteristics of the grating and how it is placed into the spectrograph.

Thus, a spectrometer can be constructed where each wavelength band to can lie on a single pixel of a CCD array.[3] This allows the maximum intensity to be measured for the band and analyzed as a discrete spectrum.

6 Experimental Procedure

6.1 Required Specifications of the Iodine Cell

A central piece of the technique described in this article is the iodine cell which imposes a forest of spectral lines onto the stellar spectrum. The background grid that the cell provides the spectrum analysis spans a wavelength range of 500 to 620 nanometers, which matches closely to the necessary range for late-type stars (Merline 1985). During observations, the cell must be maintained at a constant temperature of $50 \pm 0.1^{\circ}$C to ensure a gaseous state with constant pressure is achieved. The cell must be mounted directly over the spectrometer's entrance slit, ensuring that only star light sent into the spectrometer has the iodine spectrum imposed on it. The construction of the iodine cell is simple and can be completed by any chemistry lab equip with a glass blower. For details on construction of the cell, see Marcy & Butler's 1992 paper, *Precision Radial Velocities with an Iodine Absorption Cell.*

6.2 Measuring the Spectrum of the Gas Cell

In order for the iodine cell to be used as intended, the spectrum of I_2 at conditions matching that of a normal observation must be well understood. To achieve this, the use of a extremely high resolution spectrometer must be used on the iodine cell. A favorite spectrometer for many researchers is the Kitt Peak National Observatory's Fourier Transform Spectrometer (FTS) at the McMath Solar Telescope. The resolution of the spectrometer is $R = 10^6$ with a S/N ratio of 700 (Butler *et al.* 1996). Due to the FTS's ability to render the spectrum at observation conditions with high resolution, the transmission spectrum of the iodine cell, now denoted as T_{I2}, can be stored and utilized later in the modeling process without; resulting in the measuring of the cell only once in its lifetime.

6.3 Calculating the Initial Guess for the PSF

Another key piece of information that needs to be known with high precision is the instrumental PSF. Unfortunately, this is not a simple process that can be done once for all future dates. The instrumental PSF must be obtained through a modeling process described in the next section. To lower the chances of the fitting algorithm to reside in a local minimum solution rather than a global minimum as desired, a guess close to the actual PSF must first be found. This is done in the following way. Researchers observe rapidly-rotating B-type stars. Due to their high visual magnitude and essentially featureless spectrum, these observations are similar to the conventional use of incandescent bulbs. However, the B-type stars have the added bonus of illuminating the telescope and spectrometer optics exactly the same way as other stellar observations. The PSF is the found through the comparison of the B-star iodine observations to that of the T_{I2} reference spectrum through the deconvolution and modeling method described in Valenti *et al.* (1995).

6.4 Finding the Intrinsic Stellar Spectrum

The final piece of required information, before modeling of observations through the iodine cell can be preformed, is finding the intrinsic stellar spectrum (ISS) for the observed stars. In theory, a ISS should be

[3]The reader should note that since the wavelength dependence is continuous, overlapping of the orders occur. When transferred to a discrete grid, like that or a CCD array, this overlapping is seen as a band of wavelengths at a single intensity per pixel. The range of this band depends both on the grating used and the size/spacing of each pixel on the CCD.

obtained with a extremely high resolution and low S/N spectrometer. However, in cases like the observations done at the Lick observatory, this is impossible. As such, the observed star light is allowed to pass through the telescope optics with the iodine cell removed. This spectrum will be smeared by the instrumental PSF. However, thanks to the results of the previous section, we can deconvolve the PSF out of the observation through a modified Jansson technique (Jansson 1969). If PSF observations are taken before and after the main observation, this will result in the best representation for the ISS available. This measured ISS is then over-sampled by 4X to match wavelength scales with T_{I2} through the use of cubic spline functions and is denoted as I_s.

6.5 Modeling the Observations

With knowledge of T_{I2}, the instrumental PSF, and I_s in hand, we are now able model the observations of the stars with the iodine cell in place over the spectrometer slit. We model these observations by:

$$I_{ob}(\lambda) = k[T_{I2}(\lambda)I_s(\lambda + \Delta\lambda)] * PSF \tag{31}$$

When fitted to the observations, the modeling procedure allows the Doppler shift ($z = \frac{\Delta\lambda}{\lambda}$), reference wavelengths and the normalization constant k as free parameters. It also models the PSF as 11 Gaussians with fixed positions and variable widths. The previously measured PSF is used as a best guess for the 10 free parameters to ensure that the model does not reach a local minimum before a global one. The model has its 13 free parameters fitted through a standard Marquardt non-linear least-squares (NL-LS) algorithm (Marquardt 1963). During the Lick Iodine Planet Search, this method returned an RMS between observation and the best fit model of 0.4% (Butler *et al.* 1996).

6.6 Correcting for the Relative Motion of the Observer

The above model allows us to calculate the Doppler shift parameter z, which we can relate to the radial velocity of the star by Equation 24. However, since the observations occur over long time scales, the motion of the earth about the sun must be taken into account.[4] This means that λ' must be corrected by (Lovis *et al.* 2010):

$$\lambda' = \lambda_{ob}\left(1 + \frac{\vec{k}_{ICRS} \cdot \vec{v}_{ICRS}}{c}\right) \tag{32}$$

where λ_{ob} is the observed wavelength, $\vec{k}_{ICRS}$ is the unit vector pointing from the observer to the source in the International Celestial Reference System (ICRS), and $\vec{v}_{ICRS}$ is the velocity vector of the Earth with respect to the ICRS . This information can be found through the IAU and NASA public databases. Otherwise, a numerical solution for the Kepler Problem with constants set to that of the Earth and a timing reference of the seasonal equinoxes can be used to derive $\vec{v}_{ICRS}$.

6.7 Finding Exoplanets

Once the correction for the motion of the observer has been completed and the true radial velocity of the star determined, several observations must be completed over the period of days, months or even years for each star in the survey. This allows for a build up of radial velocity data points. So long as the observations do not closely match the orbital period of the star about the barycenter, a NL-LS algorithm can be fit to the data to retrieve K and, following from that, the orbital parameters of the sub-stellar companion. The

[4]The motion of the Earth about its rotational axis can be corrected through the tracking of the telescope, now done easily with high precision.

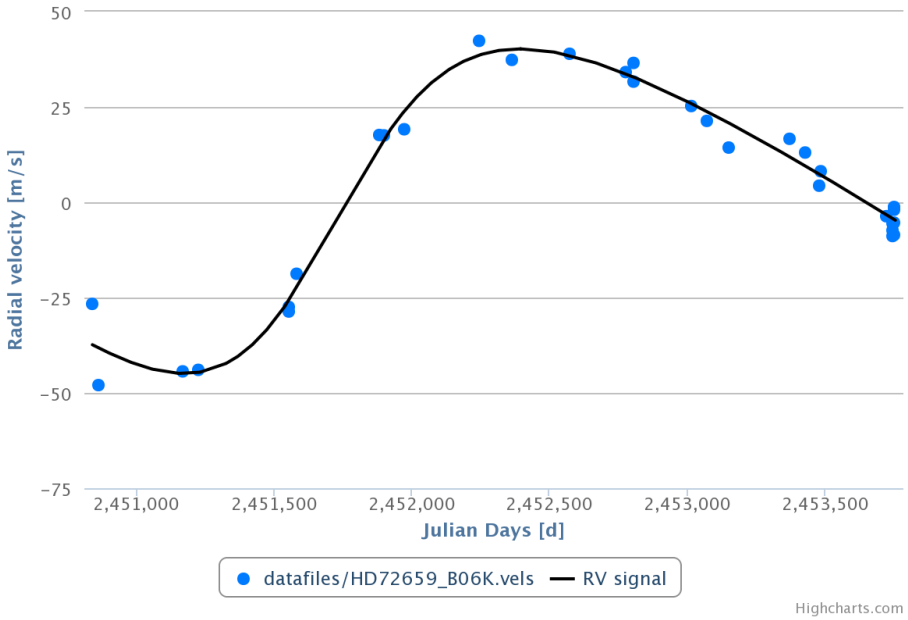

Figure 2: The radial velocity plot for HD72659 observations taken in 2003. The fit is provided by the Systemic Live tool kit.

tool kit provided by Stefano Meschiari of the McDonald Observatory at the University of Texas at Austin, *Systemic*, allows for robust analysis to be done on any radial velocity data set. This tool kit also allows for the possibility of multi-planet systems, which seem to be increasingly more common. Included below is a example of this tool's abilities.

6.7.1 HD 72659b

This section details the *Systemic Live!* tool kits ability to accurately detect exoplanets via radial velocity data. We first load the data set "HD72659_B06K" which comprises of 32 data points collected of the star HD 72659, a yellow dwarf star in the Hydra constellation of apparent magnitude is +7.48 and a distance of 168 light years. By viewing the star's power spectrum, we determine that a best guess for the period of the exoplanet causing the periodic motion of the star is around 4000 days. We add in a single planet into the model and suggest a period of 4000 days. Once all orbital parameters are selected to be fitted, the program computes the solution to the NL-LS problem. The returned graphs can be found in Figure 2 and Figure 3. The corresponding constants can be found in 1. These results were very close to those proposed by Butler *et al.* in the 2003 discovery paper.

Table 1: Systemic Live! Analysis of HD 72659b

S.M. Axis [AU]	**Period [Days]**	**Mass [M_j]**	**Orbital** e
4.5684	3653.31	3.0093	0.2689

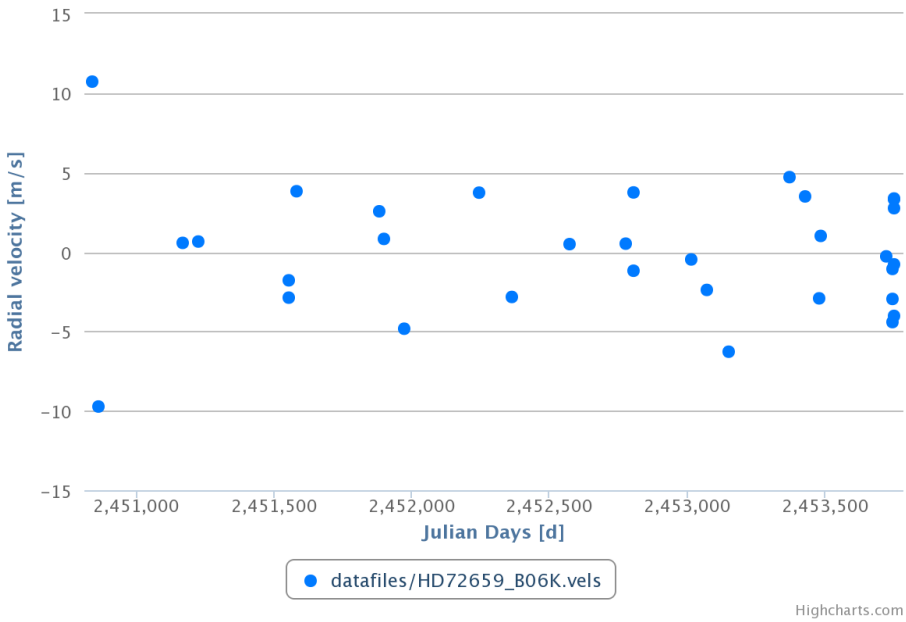

Figure 3: The residual plot of the HD72659 data-set when compared to the best-fit model of a singular companion.

7 Concluding Thoughts

In closing, it is clear from media coverage in both the scientific and public domains that exoplanets are one of the primary frontiers in astrophysics today. Increased funding in space-bound telescope missions similar to the Kepler mission are being prepped for launch across the globe. As more techniques are developed and technology improves, it the ability to detect planets within the habitable zone of Sun-like stars is likely to increase dramatically. For example, in 2003 the High Accuracy Radial Velocity Planet Searcher (HARPS) on the European Southern Observatory achieved a precision of 50 cm s^{-1}. These performances have allowed the for the ability to detect planets down to a few Earth masses. Even more impressive is the combination of other observational techniques, such as the growing popularity Transit Method, to refine radial velocity measurements to incredible levels of precision by directly measuring $\sin i$. Indeed, its is the opinion of the author and much of the scientific community that within the next few decades we discover a possible home for humanity whose conditions match the Earth almost perfectly. After all, with numerous planets orbiting around billions of stars within our Milky Way Galaxy which sits in a potentially infinite universe, it is unlikely that we live on the only pale blue dot capable of letting humanity call it home.

8 Acknowledgments

We are grateful to: the Department of Physics at Cleveland State University for facilitating the course which allowed this study to be done; the Honors Scholarship which funded J. Glaser during his years of undergraduate studies in the fields of physics and mathematics; and J. Lock for his guidance and support throughout the term and the many years of instruction previous to the start of this study.

References

[1] C. Beaugé, S. Ferraz-Mello, & T. A. Michtchenko, Research in Astronomy and Astrophysics, **12.8**, pp. 1044 (2012).

[2] R. P. Butler & G. W. Marcy, Publications of the Astronomical Society of the Pacific, **104**, pp. 270 (1992).

[3] R. P. Butler, G. W. Marcy, E. Williams, C. McCarthy, & P. Dosanjh, & S. S. Vogt, Publications of the Astronomical Society of the Pacific, **108**, pp. 500 (1996).

[4] R. P. Butler, G. W. Marcy, S. S. Vogt, D. A. Fischer, G. W. Henry, G. Laughlin, & J. T. Wright, Astrophysical Journal, **582**, pp. 455 (2003).

[5] F. V. Hessman *et al.*, arXiv.org, **1012.0707** (2010).

[6] P. A. Jansson, Journal of the Optical Society of America, **60.2**, pp. 184 (1969).

[7] D. W. Marquardt, Journal of the Society for Industrial and Applied Mathematics, **11.2**, pp. 431 (1963).

[8] S. Seager *et al.*, *Exoplanets*, 1st Ed. (University of Texas at Austin, Austin, TX, 2006), pp. 27-54.

[9] J. A. Valenti, R. P. Butler, & G. W. Marcy, Publications of the Astronomical Society of the Pacific, **107**, pp. 966 (1995).